Transactions of the Materials Research Society of Japan 29 [8] 3615-3618 (2004)

Molecular Dynamics Study on Nano Structure and Shape-memory Property of Ni-Ti Alloy

Tomohiro SATO, Ken-ichi SAITOH*, Takuya UEHARA** and Noboru SHINKE*
Mechanical Engineering Major, Graduate School of Kansai University,
3-3-35 Yamate-cho, Suita-shi, Osaka 564-8680, Japan
Fax: 81-6-6388-8785, e-mail: saitou@ipcku.kansai-u.ac.jp
* Department of Mechanical Engineering, Faculty of Engineering, Kansai University,
3-3-35 Yamate-cho, Suita-shi, Osaka 564-8680, Japan
** Department of Energy Conversion Science, Graduate School of Energy Science, Kyoto University,
Yoshida Hon-machi, Sakyo-ku, Kyoto 606-8501, Japan

By using molecular dynamics simulation (MDS), we investigate atomistic aspect of phase transformation, which is sure to lead to shape-memory effect on nano-size Ni-Ti alloy. For atomic interactions in Ni-Ti shape memory alloy (SMA), we use EAM potential function. We prepare the MDS model including surface and constrained parts, and conduct a cycle of MDSs: relaxation, loading, un-loading, heating, and cooling MDS. Starting with MDS model where the atomic configuration is in parent phase of B2 structure, complete recovery of lattice structure is observed. Lattice parameters including angle parameters of some B19' structures which are reported as martensite phase of Ni-Ti alloy and those simulated by MDS are compared. Angles around 93.3° or 97.5° agree well with known parameter. Furthermore, ratio of two distances which consist of the angle is also alike. It is concluded that martensitic transformation from B2 structure to B19' structure is induced during this reversible change of atomic rearrangement and stress-induced phase transformation is achieved.
Key words: Molecular Dynamics, Ni-Ti Alloy, EAM potential, Phase transformation, Shape Memory Property

1. INTRODUCTION

Ni-Ti alloy (so-called nitinol) is well known as shape memory alloy (SMA) and is one of the general-using materials in engineering. Generally speaking, SMA is very successful as functional material. Selected stoichiometry, heat treatment, and manufacturing process of SMA can change properties so that the product takes not only shape memory effect (SME) but also super elasticity effect, damping effect, and so on. These characteristics have attracted researchers and they invented many applications of mechanical element such as actuators, mobile phone antennas, and vibration dampers. Nowadays, SMA is developing as thermal-driving thin films actuator. On the other hand, it seems that insufficient knowledge on the complicated properties of SMA prevents us from developing more useful applications which will be taken full advantage of these materials. Basic studies of SMA are still needed to understand its mechanical properties clearly. Main deformation mechanism which causes SME is martensitic transformation of crystal structure. However, even in Ni-Ti, the popular SMA, its martensitic crystal structure (B19') is still controversial. One of the reasons is difficulty in experimental observation. Recently, some investigations begin determining this structure by using computational methodology. For example the total energy of crystal structure of Ni-Ti martensite phase is calculated by first-principle calculation and FLMTO[1]. It is reported that the energy of martensite phase predicted by Kudoh *et al.*(called KTMO) is the lowest at 0K. Also using first principle calculation, the other case is examined by Huang *et al.*[2]. They compare calculated results with experimental value and suggest that residual stress is important for B19' structure. At this point it is also important to clarify the mechanism of phase transformation that is a principal factor of SME. However, it is furthermore hard to observe experimentally and continuously the reversible phase change in SMA. Computational methods give much insight about these properties. Molecular Dynamics Simulation (MDS) can effectively configure the model of dynamic phase transformation, because it is a successful microscopic and dynamic method of computational mechanics. In this paper, we simulate behavior of nano size Ni-Ti model and evaluate nano structure of martensite phase by MDS. We also discuss how shape memory properties appear in nano-scale.

2. Ni-Ti ALLOY

In this section we introduce briefly details of Ni-Ti alloy. Table I shows various lattice constants of the Ni-Ti crystal structures. The Ni-Ti parent phase is the B2 (bcc-like CsCl structure). It is stable at high temperature. On the other hand, the martensite phase of Ni-Ti is monoclinic B19' structure (Fig.1) which is stable at low temperature. It is difficult to obtain single B19' crystal for examination by using X-ray diffraction. But different kinds of some unitcell in this structure are proposed by experiment or static calculations (Table I). Fig.2 shows schematically the process model of SME. By this model, we can explain basic mechanism of SME. Fig.2(A) is conformation of parent phase. By cooling this phase, the crystal starts to become martensite phase when temperature is below M_s. After temperature passes M_f (Fig.2(a)), all of the alloy become martensite phase B19' structure (Fig.2(B)). Then the alloy does not have a

Table I Comparations of lattice parameters for Ni-Ti martensite and parent (Fig.1 shows structure of B19' proposed by Otuka *et al.*)

	a[Å]	b[Å]	c[Å]	β [°]	γ[°]	b/a
Otuka *et al.*[3]	2.889	4.120	4.622	96.8		1.600(c/a)
HS [1]	2.883	4.623	4.117		96.8	1.604
MS [1]	2.885	4.622	4.120		96.8	1.602
BGKMS [1]	2.884	4.665	4.110		98.10	1.618
KTMO [1]	2.898	4.646	4.108		97.76	1.603
USPP-LDA [2]	2.861	4.600	3.970		97.8	1.608
USPP-GGA [2]	2.929	4.686	4.048		97.8	1.600
YCH-LDA [2]	2.892	4.598	4.049		97.8	1.590
Lai *et al.* [4]	2.956	4.455	4.189		93.26	1.507
B2 (parent)	3.010	4.257	4.257			1.414

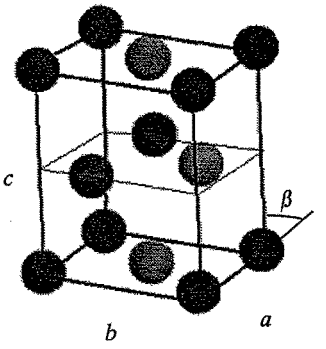

Fig.1 B19' structure

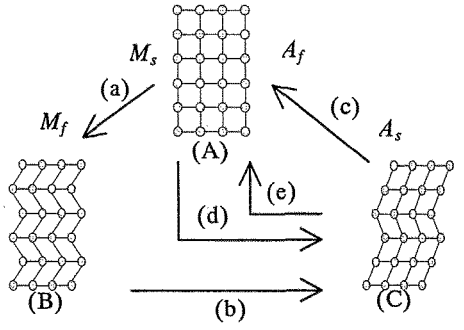

Fig. 2 Model of SME ((a) cooling, (b)(d) loading, (c) heating, (e) unloading, (A) parent, (B) martensite, (C) deformed martensite.)

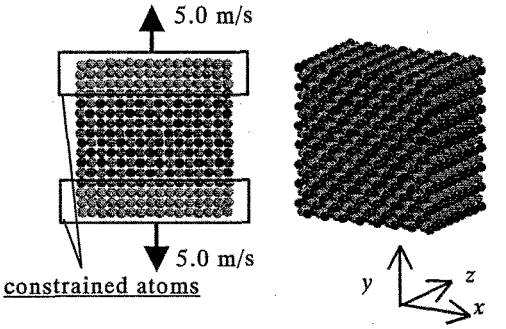

Fig. 3 Simulation model for type A (x-$[011]_{B2}$, $[100]_M$, y-$[0\bar{1}1]_{B2}$, $[001]_M$, z-$[\bar{1}00]_{B2}$,$[010]_M$, darker atom is Ni, lighter atom is Ti.)

single crystal, it is polycrystal with variants which appear with self-accommodation. Because of this function, we cannot tell Fig.2(A) from Fig.2(B) in macroscopic scale. When the martensite is loaded (Fig.2(b)), it is strained and left an apparent plastic deformation (Fig.2(C)). Heating this deformed structure through temperature range from A_s to A_f (Fig.2(c)), it recovers its original parent B2 phase. Super elasticity effect is also shown in Fig.2(d,e). In the case of Ni-Ti stress-induced martensite transformation occurs by loading at temperature above A_f (Fig.2(d)). Unloading lets this forced alloy recover its original shape (Fig.2(e)). In these two processes, all the atomic bonds in it do not always recover initial state. Thus, this material loses strength in repeated loadings.

3. SIMULATION METHOD

3.1 Simulation model

Fig.3 shows a simulation model of Ni-Ti single crystal in B2 structure which we choose as a initial state. The model shown here consists of 2176 atoms (52.9 at%Ni), which we call type A. We also prepare another model (type B) which has 11774 atoms (51.7 at%Ni). Both models show the same crystalline orientation, where each coordinate axes, (x,y,z) , correspond to indicates $[011]_{B2}$, $[0\bar{1}1]_{B2}$, and $[\bar{1}00]_{B2}$, respectively. TableII shows size and conditions of two models.

Table II Condition of simulation model

Type	A	B
Number of atoms	2176	11774
Stoichiometry[at%Ni]	52.9	51.7
Number of constrained atoms	816	2436
Displacement speed [m/s]	5.0	15.0
Size of model [nm]		
x	3.19	5.75
y	3.19	5.96
z	2.41	4.21

3.2 Interatomic potential function

We use EAM (embedded atom method) potential function which is proposed by Lai *et al.*[2]. Lattice stability of some Ni-Ti phases and effect of chemical composition are studied by this potential. The total energy of the system E is given by

$$E = \sum_i \left\{ \sum_{j \neq i} A_{\alpha\beta} \exp\left[-p_{\alpha\beta}\left(\frac{r_{ij}}{d_{\alpha\beta}} - 1 \right) \right] - \sqrt{ \sum_{j \neq i} \xi_{\alpha\beta}^2 \exp\left[-2q_{\alpha\beta}\left(\frac{r_{ij}}{d_{\alpha\beta}} - 1 \right) \right] } \right\}$$

-[1].

Table III shows potential parameters. In this function, a and β are substituted by atomic species, that is, nickels, titaniums, or combinations of these two elements. The parameter d is a nearest-neighbor distance, and r_{ij} is the actual distance between i-atom and j-atom. A, ξ, p, and,

Table III Parameter of potential function [4]

parameter	unit	Ni-Ni	Ti-Ti	Ni-Ti
d	Å	2.49	2.95	2.607
A	eV	0.104	0.153	0.3
ξ	eV	1.591	1.879	2.48
p		11.198	9.253	7.9
q		2.413	2.513	3.002

Table IV Simulation condition for type A

Stage	Time [ps]	Temperature [K]
1 Relaxation	20.0	10
2 Tensile	25.0	10
3 Relaxation	20.0	10
4 Compressive	6.0	10
5 Relaxation	20.0	10
6 Heating	40.0	10→1000
7 Relaxation	20.0	1000
8 Cooling	40.0	1000→10
9 Relaxation	20.0	10

q are determined as follows. For the case of $\alpha = \beta$ fitting is performed on the cohesive energy, lattice parameters, elastic constants and the unrelaxed vacancy formation energy at 0K. For $\alpha \neq \beta$, fitting is done by the B2 phase at 0K.

3.3 Simulation condition

Calculations are set up for several stages. Details are shown in Table IV. By completing all stages, the Ni-Ti model comes back to the original conditions. In loading calculation (stage 2), some atoms in the end of the model are constrained to move at constant displacement speed shown in Table II. These atoms exist within 0.5nm range from x-z surfaces along y direction and are given displacement speed toward only y direction as shown in Fig. 3. From the beginning of stage 2, we keep constraining these atoms. Stress is evaluated by averaging all the atomic stress in each component, using definition in literature [4]. On monitoring normal stress in y direction, when it indicates the yield point, we stop loading and move to stage 3. In unlading stage, constrained atoms are given the same speed as stage 2, in opposite directions until 0 stress situation is detected. On relaxing, they have no velocity in all directions. To control temperature, the conventional velocity scaling method is adopted. When heating and cooling the system, temperature increases or decreases linearly with time progress.

4. RESULTS AND DISCUSSION

Fig.4 shows a stress-time relation through all the simulation stages. Behavior of type A model at several stages is shown in Fig.5. At loading stage, elastic deformation is induced by normal stress component in tensile direction. In between Fig.5(a) and (b), small deformation is confirmed. As remarkable phenomena at stage 3 (Fig.5(c)), the stress decreases rapidly on relaxation, where deformation propagates like a slip. When detecting 0 stress situation in stage 4, a kind of residual strain remains in the model (Fig.5(d)). From heating process to cooling process, stress keeps rising. In the temperature range from 400K to 730K, stress increases rapidly. That is alike increasing stress at constant strain in tensile loading testing of actual SMA. During those thermal processes, we can observe recovering of lattice structure in the model, that means rearrangement of atoms (Fig.5(e)(f)). Tendency in stress curve of type B model is similar to that of type A until

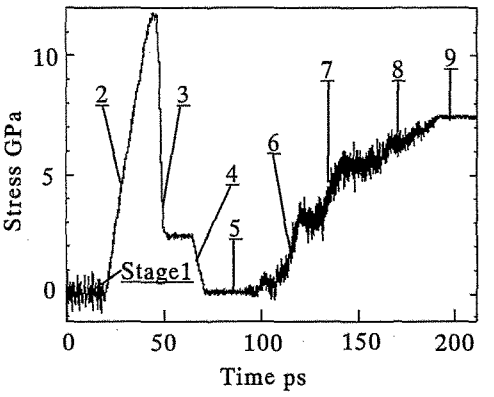

Fig. 4 Stress-time relation of type A (normal stress component in tensile direction is shown.)

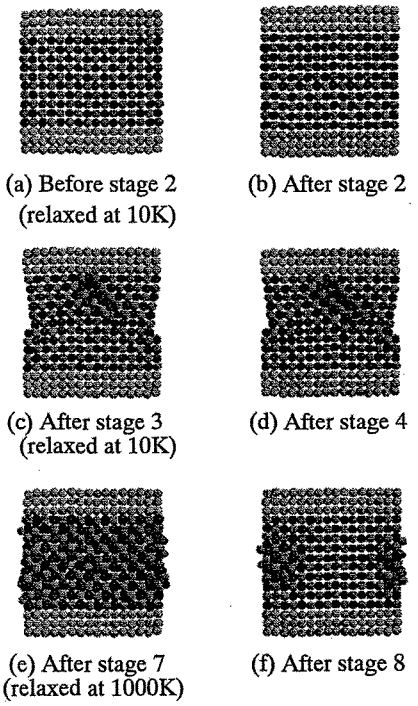

(a) Before stage 2 (relaxed at 10K)
(b) After stage 2
(c) After stage 3 (relaxed at 10K)
(d) After stage 4
(e) After stage 7 (relaxed at 1000K)
(f) After stage 8

Fig.5 Behavior of model

stage 5. However, atomic configurations of deformed parts in stage 3 and the way of the stress increasing in stage 6,7,8 are slightly different. This suggests that positions of phase change are influenced by model size.

To clarify shape-memory properties from these features of the models, we observe atomistic changes of positions, velocities, and other evaluations for type A. At first, we investigate distributions of distance between two atoms and of angle which is made up of three atoms. Results of the distribution are shown in Fig.6, Fig.7 and Fig.8. These analyses make us understand how phase transition occurs. Distribution of atoms before loading is shown in Fig.6(a). Several peaks indicate lattice distance and nearest neighbor distatance in B2 structures of Ni-Ti. After the model is strained at 0.078 by tensile loading, some peaks move to the positions which indicate B19' structure (Fig.6(b)). This appearance of martensite structure tells us that some lattice distances and angles

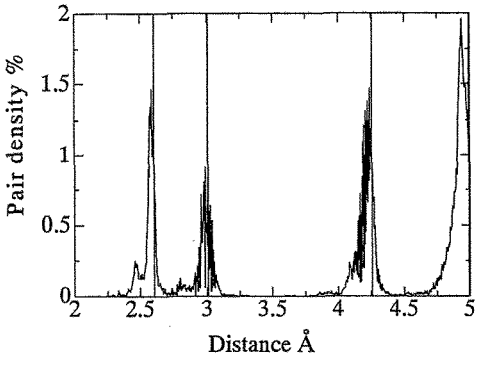

(a) Before stage 2

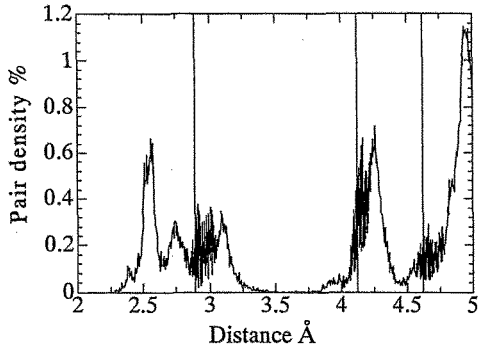

(b) After stage 2

Fig. 6 Lattice distance-pair density ((a) Vertical lines (distance = 2.607, 3.010, 4.257) indicate nearest-neighbor distance and lattice parameter of B2 (the last line in Table I). (b) Vertical lines (distance = 2.889, 4.120, 4.622) indicate lattice parameters of B19' (the first line in Table I).)

(Table II) are important guide to detect it. Distribution of angles is shown in Fig.7, where by using law of cosines, we caluculate angles among neighbor atoms. By comparing the peaks before and after loading (Fig.7(a) and (b)), they certainly shift. In these peaks of distribution, the angle which B19' structure normally has is included. Based on these results, we narrow down viewing ranges around the value of β or γ B19' structure must have. Fig.8 shows the relation between the number of triplets and the ratio of two distances which consist of triplets' angle. Angle range is between 96.5° and 98.5° or between 92.5° and 93.5°. Distance range for detecting a is between 2.75Å and 4.70Å, and that for detecting b is between 4.55Å and 4.70Å. The value b/a agrees well with that listed in Table I. This shows the evidence that transformation from parent phase to martensite phase occurs.

5. CONCLUSION

Investigating nano structure of Ni-Ti alloy by atomistic model and MDS is effective to make clear shape-memory property. In heating process, large increasing of stress occurs like actual SMA subjected to constant strain. In loading simulation, it is detected that lattice parameters of B2 parent phase shift to those of B19' martensite phase already proposed.

6. REFERENCE

[1] M. Sanati, R. C. Albers and F.J. Pinski, *Phys.Rev.B.*, **58**, 13590-13593 (1998).
[2] X. Huang, G. J. Ackland and K. M. Rabe, *Naturer Materials.*, **2**, 307-311 (2003).
[3] T.Saburi, S.Nenno, *Proc.Int.Conf.Solid.Solid Phase Transform.1981.*, 1455-1479 (1982).
[4] W.S.Lai B. X. Liu, *J.Phys.Condens.Matter.*, **12**, L53-L60 (2000).
[5] Born.M., Huang.K., *Dynamical Theory of Crystal lattices*, Oxford, 129 (1954).

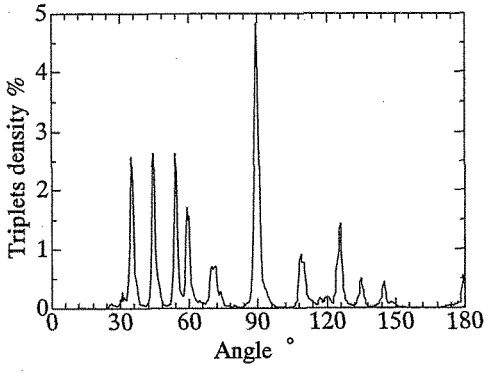

(a) Before stage 2

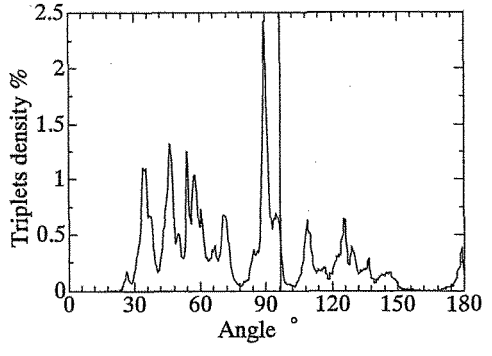

(b) After stage 2

Fig. 7 Angle-triplets density ((b) Vertical line indicates 96.8° which B19' statically has (the first line in Table I).)

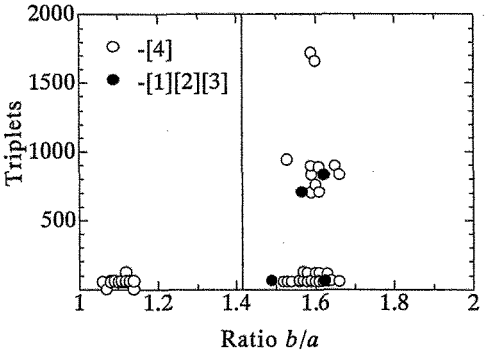

Fig.8 Ratio of two distances-triplets of three atoms (triplets' angle between 96.5° and 98.5°, ○(Reference,[1][2][3]), between 92.5° and 93.5°, ●(Reference,[4]), including β or γ of B19' . Vertical line is 1.414 for B2 parent phase. (the first and last line in Table I).)

(Received October 15, 2003; Accepted March 10, 2004)